Prepared for
Office of Naval Research
Contract No. N00014-69-A-0200-4048

California University, Los Angeles

UCLA-ENG-7414
FEBRUARY 1974

OPTIMUM DESIGN OF RING STIFFENED CYLINDRICAL SHELLS

A.J. BRONOWICKI
R.B. NELSON
L.P. FELTON
L.A. SCHMIT, JR.

UCLA • SCHOOL OF ENGINEERING AND APPLIED SCIENCE

UNCLASSIFIED

SECURITY CLASSIFICATION OF THIS PAGE *(When Data Entered)*

REPORT DOCUMENTATION PAGE		READ INSTRUCTIONS BEFORE COMPLETING FORM
1. REPORT NUMBER	2. GOVT ACCESSION NO.	3. RECIPIENT'S CATALOG NUMBER
4. TITLE *(and Subtitle)* OPTIMUM DESIGN OF RING STIFFENED CYLINDRICAL SHELLS		5. TYPE OF REPORT & PERIOD COVERED 6. PERFORMING ORG. REPORT NUMBER UCLA-ENG-7414
7. AUTHOR(s) Allen J. Bronowicki Lucien A. Schmit, Jr. Richard B. Nelson Lewis P. Felton		8. CONTRACT OR GRANT NUMBER(s) Contract No. N00014-69-A-0200-4048
9. PERFORMING ORGANIZATION NAME AND ADDRESS Mechanics and Structures Department School of Engineering and Applied Science University of California, Los Angeles, Cal. 90024		10. PROGRAM ELEMENT, PROJECT, TASK AREA & WORK UNIT NUMBERS
11. CONTROLLING OFFICE NAME AND ADDRESS Procuring Contracting Officer Office of Naval Research Department of the Navy, Arlington, Va. 22217		12. REPORT DATE February 1974 13. NUMBER OF PAGES 29
14. MONITORING AGENCY NAME & ADDRESS *(if different from Controlling Office)* Director, Office of Naval Research Branch Office-Pasadena 1030 East Green Street Pasadena, Calif. 91101		15. SECURITY CLASS. *(of this report)* 15a. DECLASSIFICATION/DOWNGRADING SCHEDULE
16. DISTRIBUTION STATEMENT *(of this Report)*		
17. DISTRIBUTION STATEMENT *(of the abstract entered in Block 20, if different from Report)*		
18. SUPPLEMENTARY NOTES		
19. KEY WORDS *(Continue on reverse side if necessary and identify by block number)* Structural design, optimal; Shells, cylindrical; Vibration; Buckling		

20. ABSTRACT *(Continue on reverse side if necessary and identify by block number)*

This report deals with the optimum structural design of circular cylindrical shells reinforced with identical uniformly spaced T-ring stiffeners, and subjected to external pressure loading. The optimization problems considered are of three types: (1) minimum-weight designs, (2) design for maximum separation of the lowest two natural frequencies, and (3) design for maximum separation of the lowest two natural frequencies which have primarily axial content. Gross buckling is precluded by specifying a minimum natural frequency, and

DD FORM 1 JAN 73 1473 EDITION OF 1 NOV 65 IS OBSOLETE
S/N 0102-014-6601

SECURITY CLASSIFICATION OF THIS PAGE *(When Data Entered)*

20. additional behavioral constraints preclude yielding or buckling of panels, T-ring stiffeners, and web and flange instabilities within each T-ring. Analysis is based on use of an equivalent orthotropic shell model, and optimization is accomplished through use of a sequential unconstrained minimization technique. Examples indicate that a small increase in weight above optimum (minimum) values can result in relatively large increases in frequency separation, and that maximum frequency separation is obtained when second and third lowest frequencies approach each other.

UCLA-ENG-7414
FEBRUARY 1974

OPTIMUM DESIGN OF RING STIFFENED CYLINDRICAL SHELLS

Allen J. Bronowicki
Richard B. Nelson
Lewis P. Felton
Lucien A. Schmit, Jr.

Prepared for
Office of Naval Research
Contract No. N00014-69-A-0200-4048

Mechanics and Structures Department
School of Engineering and Applied Science
University of California
Los Angeles, California 90024

ACKNOWLEDGMENT

The research described in this report was performed under Office of Naval Research Contract No. N00014-69-A-0200-4048.

ABSTRACT

This report deals with the optimum structural design of circular cylindrical shells reinforced with identical uniformly spaced T-ring stiffeners, and subjected to external pressure loading. The optimization problems considered are of three types: (1) minimum-weight design, (2) design for maximum separation of the lowest two natural frequencies, and (3) design for maximum separation of the lowest two natural frequencies which have primarily axial content. Gross buckling is precluded by specifying a minimum natural frequency, and additional behavioral constraints preclude yielding or buckling of panels, T-ring stiffeners, and web and flange instabilities within each T-ring. Analysis is based on use of an equivalent orthotropic shell model, and optimization is accomplished through use of a sequential unconstrained minimization technique. Examples indicate that a small increase in weight above optimum (minimum) values can result in relatively large increases in frequency separation, and that maximum frequency separation is obtained when second and third lowest frequencies approach each other.

SYMBOLS

t_s	Thickness of shell skin (in)
t_ϕ	Thickness of frame web (in)
t_f	Thickness of frame flange (in)
d_ϕ	Depth of frame web (in)
d_f	Width of frame flange (in)
ℓ_x	Spacing of frames (in)
W	Normalized mass of structure
ρ_s	Mass density of structural material ($slug/in^3$)
L	Total length of structure (in)
R	Radius to mid-surface of skin (in)
P	Hydrostatic pressure (psi)
T	Kinetic energy
x,ϕ,z	Shell coordinate system
u,v,w	Midsurface displacements
$\tilde{u},\tilde{v},\tilde{w}$	Displacements of an arbitrary point
$\{A\}_i$	Eigenvector of ith natural frequency
ω	Natural frequency
n,m	Wave numbers
τ	Time (sec)
$[K]$	Stiffness matrix
$[K_G]$	Geometric stiffness matrix
$[M]$	Mass matrix
σ_y	Yield stress (psi)
$\sigma_{f_{cr}}$	Critical flange buckling stress (psi)
$\sigma_{w_{cr}}$	Critical web buckling stress (psi)
F	Objective function

$\underline{x}$	Vector of design variables
$g(\underline{x})$	Design constraint
q	Number of design variables
P_{cr}	Critical pressure for buckling of skin (psi) between frames
ω_{min}	Minimum allowable natural frequency of vibration in vacuo (Hz)
E	Young's modulus
ν	Poisson's ratio
ℓ	Unsupported length of shell plating (in)
W_{max}	Maximum allowable normalized structural mass
$\Phi(\underline{x})$	Composite objective function
ε	Constant for use in computing extended penalty function
r	Positive scalar quantity
$\underline{s}$	Direction vector for uni-directional search

INTRODUCTION

Although a wealth of literature exists for the static, dynamic and stability analyses of stiffened shells of revolution subjected to various applied loads, with the majority of these studies devoted to cylindrical shells, the work of Schmit and Morrow [1] serves as a pioneering effort toward the introduction of structural optimization concepts into the design of stiffened cylindrical shells. In this reference a cylindrical shell, reinforced with longitudinal and ring stiffeners, each with rectangular cross section, was designed to carry a number of independently applied sets of static loads with minimum structural weight. The shell was constrained against overall (system) buckling, panel and stiffener buckling, and also against material yield. The mathematical model which formed the basis for the stress and buckling analyses was an equivalent homogeneous orthotropic shell; i.e., the discrete stiffeners and skin stiffness properties were incorporated in the orthotropic elastic shell stiffness properties. This theory, a 3rd order Flugge-Lur'e-Byrne type theory, proved adequate provided the stiffener spacing and cross sectional dimensions were sufficiently small to permit the smoothing operation inherent in the orthotropic shell model.

In a more recent study, Pappas and Allentuch [2,3] investigated the minimum-weight design of ring stiffened cylindrical shells, subjected to a number of static applied load conditions. In this study, the ring stiffeners were T-shaped rather than rectangular. The structural analyses of general instability, localized panel instability, and stiffener instabilities were based on buckling formulas contained in Ref. [4], along with the appropriate stress limits.

The subject of this report is, in essence, a structural optimization study which employs both a combination and an extension of the structural

models in Refs. [1-3]. In the present study, three somewhat different structural optimization problems have been formulated. In the first, the minimum-weight design of a ring stiffened cylindrical shell subjected to several applied static loads is considered. The structure is constrained against all of the buckling modes considered in Refs. [2,3] although for some of the modes, the constraint equations differ. Further, the structure is constrained against in vacuo natural vibrations below a specified frequency limit. In the second formulation the shell is designed to maximize the separation between the lowest two in vacuo natural frequencies, while being constrained against buckling and yield behavior as specified in the first design problem, and while having a weight less than a prescribed maximum. The third formulation is similar to the second, with the distinction that the frequencies being separated are the two lowest which have primarily axial content.

This optimization study, in either the weight minimization form or the frequency separation forms, represents a considerable advance beyond previous characterizations of the optimization problem. The structural model in this study is based on the equivalent orthotropic shell model of Ref. [1], with dynamic effects added. This representation, although somewhat imprecise in its ability to model a ring stiffened shell, has proved invaluable in providing an economical and yet reasonably complete initial structural representation for use in the optimization studies performed. A more detailed description of the mathematical model, and a summary of the results of this research, are presented in the following sections.

ANALYSIS OF STIFFENED SHELLS

The investigation detailed in this report is concerned with the optimum structural design of circular cylindrical shells with uniformly spaced T-ring stiffeners (Fig. 1) and subjected to several different applied loading conditions typical of submerged vessels, namely (1) specified external pressure (or vessel depth), (2) specified axial compressive loadings, and (3) applied static loads associated with vessel motion. Design variables, shown in Fig. 1, are skin thickness (t_s), stiffener web thickness (t_ϕ), web depth (d_ϕ), spacing (ℓ_x), flange width (d_f), and flange thickness (t_f). Radius (R), length (L), and the material properties are assumed to be preassigned parameters.

All of the research performed to date has employed the simplified orthotropic shell model given in [1] in the calculation of the natural frequencies of vibration and in the overall (system) buckling analysis. This idealization has offered the advantage of mathematical simplicity and the disadvantage of a somewhat limited modeling capability*, but it has provided an economical initial structural representation for use in the optimization studies.

In order to analyze the dynamic response of the cylinder in Fig. 1, it is hypothesized (as in Ref. 1) that the frames and skin act as a unit according to the Bernoulli-Euler deformation assumption as extended through the Flugge-Lur'e-Byrne theory, and that the stiffness and inertia properties of the frames are uniformly distributed over the length of the cylinder. It is then possible to express the kinetic energy of the shell in the form

$$T = \frac{\rho_s}{2} \int_0^L \int_0^{2\pi} \int_t (\dot{\tilde{u}}^2 + \dot{\tilde{v}}^2 + \dot{\tilde{w}}^2) \, dz \, d\phi \, dx \qquad (1)$$

*The model gives a very accurate representation of the structural behavior provided the characteristic wavelengths of the modes of vibration (or of the static displacements) are very long compared to both the ring spacing and ring cross-sectional dimensions.

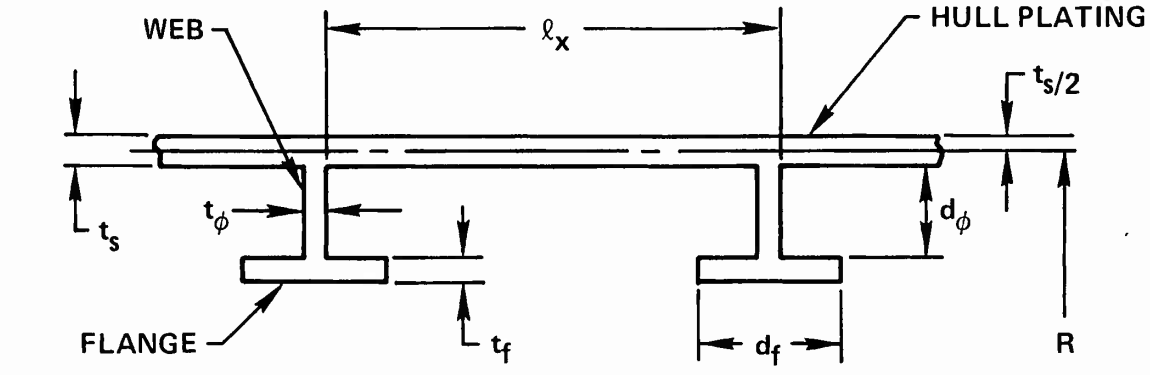

(b) FRAME AND SKIN DETAIL

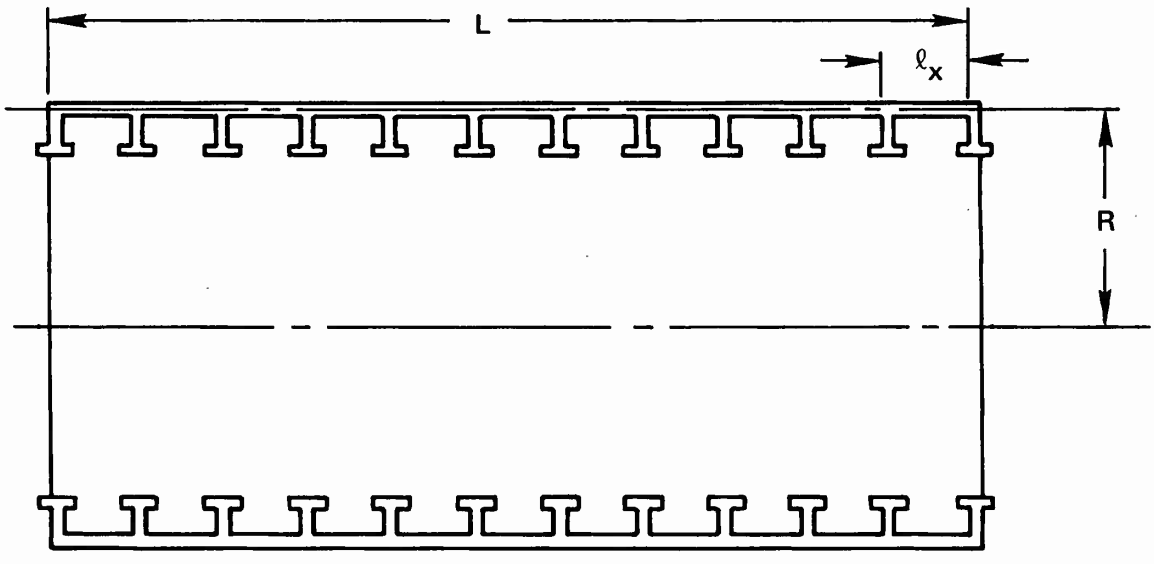

(a) HULL SEGMENT CROSS–SECTION

Figure 1. Typical Hull Segment Cross Section (from Ref. 2).

where $\tilde{u}$, $\tilde{v}$ and $\tilde{w}$ are the displacements of an arbitrary point in the structure in the x, ϕ, and z directions, respectively (Fig. 2), and are given by [1]

$$\tilde{u} = u - z\frac{\partial w}{\partial x} \tag{2a}$$

$$\tilde{v} = (1-\frac{z}{R})v - \frac{z}{R}\frac{\partial w}{\partial \phi} \tag{2b}$$

$$\tilde{w} = w \tag{2c}$$

where u, v and w are the displacements of the shell's mid-surface. From the kinetic energy the inertia terms in the appropriate equations of motion are obtained by use of Hamilton's principle. These terms are appended to the equations of static equilibrium for the stiffened shell in [1], which also contain the influence of destabilizing forces.

Assuming that the external loads give rise to circumferential and longitudinal compressive forces per unit length of magnitude PR and PR/2, respectively, where P is hydrostatic pressure, then the combination of inertia, static, and destabilizing forces leads to the following three coupled partial differential equations of motion.

$$N_x' + \frac{1}{R}N_{\phi x}^* - \frac{P}{R}(u^{**} - Rw') - \frac{PR}{2}u'' = p_x \tag{3a}$$

$$\frac{1}{R}N_\phi^* + N_{x\phi}' - \frac{1}{R}M_{x\phi}' - \frac{1}{R^2}M_\phi^{\cdot} - \frac{P}{R}(v^{**} + w^*) - \frac{PR}{2}v'' = p_y \tag{3b}$$

$$M_x'' + \frac{1}{R}M_{\phi x}^{*\prime} + \frac{1}{R}M_{x\phi}^{\prime *} + \frac{1}{R^2}M_\phi^{**} + \frac{1}{R}N_\phi + \frac{P}{R}(v^* - w^{**} - Ru' - \frac{R^2}{2}w'') = p_z \tag{3c}$$

where

$$p_x = \rho_s \int_t [\ddot{u} - z\ddot{w}'](1 - \frac{z}{R})dz \tag{4a}$$

$$p_y = \rho_s \int_t [(1 - \frac{z}{R})^2\ddot{v} - (1 - \frac{z}{R})(\frac{z}{R})\ddot{w}^*](1 - \frac{z}{R})dz \tag{4b}$$

$$p_z = \rho_s \int_t [\ddot{w} + z\ddot{u}' + (1 - \frac{z}{R})(\frac{z}{R})\ddot{v}^* - (z)^2\ddot{w}'' - (\frac{z}{R})^2\ddot{w}^{**}](1 - \frac{z}{R})dz \tag{4c}$$

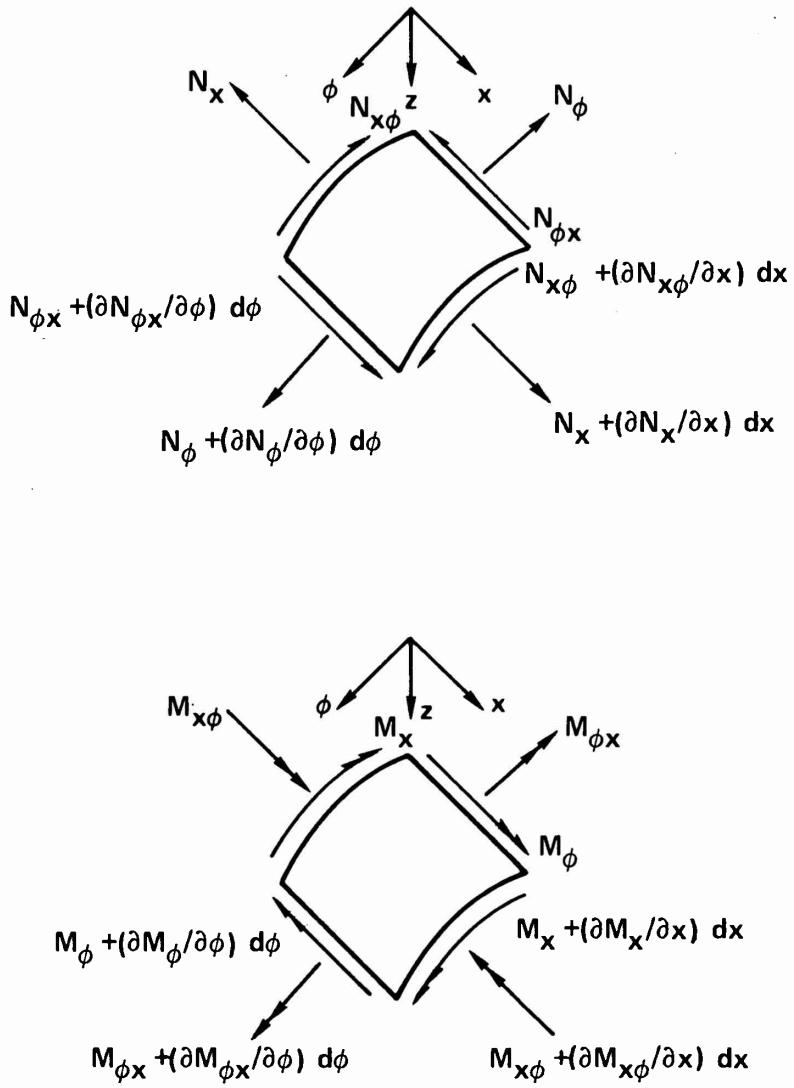

Figure 2. Force Resultants and Coordinate System.

and where $\dot{(\ )}$ denotes $\frac{\partial(\ )}{\partial\tau}$, $(\ )'$ denotes $\frac{\partial(\ )}{\partial x}$, $(\ )^*$ denotes $\frac{\partial(\ )}{\partial\phi}$ and $\int_t (\ )dz$ is the integral through the thickness of the shell and frame. The forces M and N may be expressed in terms of the mid-surface displacements u, v and w (see Appendix I) so that Eqs. (3) can be expressed in terms of displacements only.

Under the assumption that the boundary conditions are of the simple support type, then the solution to these equations takes the form

$$\begin{aligned} u &= A_1 \sin n\phi \cos \frac{m\pi x}{L} \sin \omega\tau \\ v &= A_2 \cos n\phi \sin \frac{m\pi x}{L} \sin \omega\tau \\ w &= A_3 \sin n\phi \sin \frac{m\pi x}{L} \sin \omega\tau \end{aligned} \tag{5}$$

where $n = 0,1,2,\ldots$ and $m = 1,2,\ldots$.

Substitution of Eqs. (5) into Eqs. (3) gives the algebraic eigenvalue problem

$$([K] - P[K_G] - \omega^2[M])\{A\} = \{0\} \tag{6}$$

where the stiffness, "geometric" stiffness, and mass matrices are [K], $[K_G]$ and [M], respectively, and are given in Appendix I.

It should be noted that the sine and cosine dependencies on the angle ϕ, and the similar dependencies on the axial variable x, could have been interchanged without influencing the matrices in Eq. (6) for $n > 0$. The $n = 0$ case as given in Eq. (6) is actually a combination of the solution form in Eqs. (5) (pure torsion) and the similar form with sine and cosine terms (with argument zero) interchanged (torsionless motion).

Since the algebraic eigenvalue problem for given values of m, n and P is of only rank three, its solution for the natural frequencies (eigenvalues) and associated modes (eigenvectors) is accomplished without difficulty.

In the portion of the structural optimization research wherein the structure was designed for the greatest separation of the lowest two axial-type vibratory modes, the modes with $A_1 = 1$, and A_2, $A_3 < 1$ were termed "axial." In order to prevent any general buckling from occurring, all the frequencies associated with

values n = 0,...,6, m = 1,...,6 were retained and forced to exceed a prescribed minimum ω_{min}.

In addition to this gross buckling, it is necessary to be able to detect the occurrence of several additional modes of "local" failure. These local failure modes consist of panel (inter-ring) yielding or buckling and yielding or buckling of the webs and/or flanges of the stiffener rings.

Panel (skin) yielding will be precluded, according to the Von Mises criterion, provided

$$(\sigma_\phi^2 - \sigma_\phi\sigma_x + \sigma_x^2)^{1/2} \leq \sigma_y \tag{7}$$

where σ_y = material yield stress in uniaxial loading, and σ_ϕ and σ_x are in-plane stresses normal to the surfaces of the element in Fig. 2. From Ref. [4] the maximum bending stresses in the panels due to external pressure are

$$\sigma_\phi = -\frac{PR}{t_s}[1 + \Gamma(H_n + \nu H_E)] \tag{8a}$$

$$\sigma_x = -\frac{PR}{t_s}(1/2 + \Gamma H_E) \tag{8b}$$

where Γ, H_E, and H_n are load factors defined in Appendix II.

A suitable approximate formula [4] for the critical external pressure which will cause panel buckling is

$$P_{cr} = 2.42E(t_s/D)^{5/2} / \{(1-\nu^2)^{3/4}[(\ell/D) - 0.45(t_s/D)^{1/2}]\} \tag{9}$$

where $\ell = \ell_x - t_\phi$ is the unsupported length of a panel, and D = 2R.

Again following Ref. [4], the maximum compressive stress in the rings may be taken as

$$\sigma_c = -PRQ/A \tag{10}$$

where $A = t_s t_\phi + t_\phi d_\phi + t_f d_f$, and Q is a load factor defined in Appendix II. The magnitude of σ_c must be less than the yield stress, σ_y, and also less than the critical values of compressive stresses at which the flange or web will

buckle. Assuming that the web and flange are infinitely long rectangular plates, that the web is simply supported along all edges, and that the flange is simply supported along three sides and free on one edge (all conservative assumptions), then the critical stresses for buckling of the flange and web, respectively, are [5]

$$\sigma_{f_{cr}} = \frac{0.506\pi^2 E}{12(1-\nu^2)}[2t_f/(d_f-t_\phi)]^2 \tag{11a}$$

$$\sigma_{w_{cr}} = \frac{4\pi^2 E}{12(1-\nu^2)}[t_\phi/d_\phi]^2 \tag{11b}$$

It should be noted that Eq. (10) neglects any effects of eccentricity in the circularity of the cylinder and of lateral-torsional stiffener buckling on the compressive stress in the rings.

FORMULATION OF OPTIMIZATION PROBLEM

As indicated in the Introduction, the optimization problem takes the following three alternative forms:

I. Find the minimum-weight design of the stiffened cylindrical shell subjected to the applied loads described previously and constrained against overall (system) buckling, panel (inter-ring) buckling, T web and/or flange buckling, panel and/or ring yield. The shell is also required to possess a lowest natural frequency (in vacuo) greater than a specified minimum.

II. Find the structural design which maximizes the separation between the lowest two natural frequencies of vibration (in vacuo) for the stiffened cylindrical shell subjected to the applied loads described previously and constrained against overall (system) buckling, panel (inter-ring) buckling, T web and/or flange buckling, panel and/or ring yield. The shell is also required to possess a lowest natural frequency greater than a specified minimum, and a structural weight less than a prescribed maximum.

III. Find the structural design which maximizes the separation between the lowest two natural frequencies of vibration (in vacuo) which have primarily axial content for the stiffened cylindrical shell subjected to the applied loads described previously and constrained against overall (system) buckling, panel (inter-ring) buckling, T web and/or flange buckling, panel and/or ring yield. The shell is also required to possess a lowest natural frequency greater than a specified minimum and a structural weight less than a prescribed maximum.

Each of these problems has the form of an inequality-constrained optimization problem, which may be solved by any of a number of mathematical programming algorithms. The particular method of solution chosen for this work is the Sequential Unconstrained Minimization Technique (SUMT) in which the optimum

structural design problem (in either form I, II, or III) is converted into a sequence of unconstrained problems [6] by means of so-called "penalty functions."

In this technique, it is required to find a vector $\underline{x}^T = \{x_1 x_2 \ldots x_i \ldots x_q\} \equiv \{t_s t_\phi d_\phi \ell_x d_f t_f\}$, the components of which are the design variables, such that a specified function of these variables, $F(\underline{x})$, is extremized while satisfying a set of constraints of form $g_k(\underline{x}) \geq 0$, $k = 1,\ldots,s$.

The "objective function," $F(\underline{x})$, takes one of three forms, depending on the optimization problem being considered. For Problem I, weight minimization,

$$F(\underline{x}) = W = \frac{2\pi\rho_s}{\pi(R+t_s/2)^2 L\rho_w}\{RLt_s + (L/\ell_x)[(R-e_\phi)t_\phi d_\phi + (R-e_f)t_f d_f]\} \quad (12)$$

where parameters e_ϕ and e_f are defined in Appendix I. In Eq. (12) $F(\underline{x})$ has been normalized by dividing shell mass by the mass of displaced water.

For Problem II, the case of separation of lowest natural frequencies, an inverse formulation is used. The separation is maximized by minimizing the inverse of the separation. For the modes being considered, an ordered list is made giving $\omega_1 < \omega_2 < \omega_3$, etc. The objective function is then

$$F(\underline{x}) = \frac{\Delta_1}{(\omega_2 - \omega_1)} \quad (13)$$

where Δ_1 is a normalization factor taken as the initial frequency separation. To separate frequencies having primarily a longitudinal deformation content (Problem III) it is necessary to examine and order frequencies in each primarily axial mode, i.e., the ones having both A_2 and A_3 smaller than A_1. The objective function is then given by

$$F(\underline{x}) = \frac{\Delta_1}{(\omega_{L_2} - \omega_{L_1})} \quad (14)$$

where the subscript L has been added to denote the longitudinal character of the shell vibration.

The number of design variables, q, is a maximum of six in this study, but may be less if certain of the design variables are fixed. Also upper and lower limits U_i and L_i, respectively, are assumed specified for each variable x_i. These upper and lower limit constraints, respectively, are written in the normalized form

$$g_i(\underline{x}) = (U_i - x_i)/(U_i - L_i) \geq 0 \qquad i = 1, \ldots, q \tag{15}$$

$$g_{q+i}(\underline{x}) = (x_i - L_i)/(U_i - L_i) \geq 0 \tag{16}$$

It is also necessary to include a geometric admissability constraint which serves to keep the frame flanges from overlapping. This is expressed in the normalized form

$$g_{2q+1}(\underline{x}) = 1 - d_f/\ell_x \geq 0 \tag{17}$$

The behavioral constraints may also be normalized. The panel yield constraint is expressed as

$$g_{2q+2}(\underline{x}) = 1 - (\sigma_\phi^2 - \sigma_x\sigma_\phi + \sigma_x^2)^{1/2}/\sigma_y \geq 0 \tag{18}$$

The frame yield, flange buckling, web buckling and skin buckling constraints, respectively, are written as

$$g_{2q+3}(\underline{x}) = 1 - |\sigma_c|/\sigma_y \geq 0 \tag{19}$$

$$g_{2q+4}(\underline{x}) = 1 - |\sigma_c|/\sigma_{f_{cr}} \geq 0 \tag{20}$$

$$g_{2q+5}(\underline{x}) = 1 - |\sigma_c|/\sigma_{w_{cr}} \geq 0 \tag{21}$$

$$g_{2q+6}(\underline{x}) = 1 - P/P_{cr} \geq 0 \tag{22}$$

Finally, to prevent gross buckling the lowest frequency, ω_1, should be greater than a specified minimum frequency, ω_{min}. This is stated in the form

$$g_{2q+7}(\underline{x}) = (\omega_1 - \omega_{min})/\Delta_2 \geq 0 \tag{23}$$

where Δ_2 is the initial value of $\omega_1 - \omega_{min}$.

For the minimum-weight design of the shell these are all the constraints required, but in order to separate frequencies two other constraints must be included. It is conceivable that large separations could be achieved, but possibly only at the expense of large increases in weight. It is therefore necessary to establish an upper bound to the mass of the structure, W_{max}. This constraint is expressed by

$$g_{2q+8}(\underline{x}) = 1 - W/W_{max} \geq 0. \tag{24}$$

The final constraint is not required in the definition of the frequency separation problems, but is convenient for numerical solution when penalty functions are utilized in the Sequential Unconstrained Minimization Technique. The most efficient unconstrained minimization methods require the computation of gradients of the objective function in order to operate. These gradients should be smooth and continuous, but experience shows that, as ω_1 and ω_2 are separated, ω_2 and ω_3 approach a common value. Eventually ω_2 and ω_3 will switch, with the result that the mode which previously represented ω_2 now represents ω_3 and vice versa. This causes discontinuity in the gradient of the objective function and subsequent difficulties with the numerical algorithm. This difficulty can be overcome simply by requiring that the second and third frequencies never be equal. This requirement is expressed as a "singularity avoidance" constraint in the two cases of frequency separation by

$$g_{2q+9}(\underline{x}) = \omega_3 - \omega_2 > 0 \tag{25}$$

or

$$g_{2q+9}(\underline{x}) = \omega_{L_3} - \omega_{L_2} > 0 \ . \tag{26}$$

In order to apply the methods of unconstrained nonlinear programming, the basic inequality-constrained problem is recast in the form of an interior

penalty function [6], the solution of which requires finding that $\underline{x}$ which minimizes

$$\Phi(\underline{x}) = F(\underline{x}) + r \sum_{j=1}^{s} P_j(\underline{x}) \tag{27a}$$

where

$$P_j(\underline{x}) = \begin{cases} 1/g_j(\underline{x}) & \text{if } g_j(\underline{x}) \geq \varepsilon \\ [2\varepsilon - g_j(\underline{x})]/\varepsilon^2 & \text{if } g_j(\underline{x}) < \varepsilon \end{cases} \tag{27b}$$

$P_j(\underline{x})$ is the so-called extended penalty function [7] which allows the use of infeasible designs in the search for an optimal feasible design. The quantities ε and r are small positive scalars and s is the number of constraints. Solving this unconstrained minimization problem for successively smaller values of r gives a series of designs which converge to a local or global optimum of $F(\underline{x})$. This procedure is referred to as the Sequential Unconstrained Minimization Technique (SUMT). Each unconstrained minimization is performed by the Davidon-Fletcher-Powell method [6]. In order to apply this algorithm it is necessary to compute the gradients of the objective function and the constraints with respect to each design variable. The mathematical complexity of this problem makes analytic calculation of partial derivatives impractical and it is found convenient to use a forward difference technique to find the gradients numerically. The success of the unconstrained minimization hinges on the ability to perform an accurate unidirectional minimization. A special hyperbolic interpolation formula was developed [6] for use with the SUMT method. A test for the minimum was developed and incorporated into the minimization algorithm which requires that a measure of normality between the direction vector $\underline{s}$, and the gradient, $\underline{\nabla\Phi}$, be less than 0.001, i.e.,

$$(\underline{s} \cdot \underline{\nabla\Phi})/(|\underline{s}| \cdot |\underline{\nabla\Phi}|) \leq 0.001 \ . \tag{28}$$

EXAMPLES

Design examples given in [3] were re-evaluated in this study for optimal performance for situations I, II or III as detailed above. In all of these designs the preassigned parameters were given the following values: $R = 198$ in., $L = 594$ in., $E = 30 \times 10^6$ lb/in.^{2}, $\sigma_y = 60 \times 10^3$ lb/in.^{2}, $\rho = 7.75 \times 10^{-4}$ slug/in.^{3}, $\nu = 0.33$ and specified pressure associated with depths of water of 1000, 2000 and 3000 ft. The prescribed minimum natural (in vacuo) frequency was taken as 12.0 Hz. Except for the dynamic effects these problems are quite similar to those in [3]. The structure was designed initially for minimum weight (problem I) for the three different operating depths. The results, given in Table 1, indicate normalized minimum weights of 0.13317, 0.22295, and 0.31922 for operating depths of 1000, 2000 and 3000 ft., respectively, values somewhat lower than reported in [3]. This occurrence is due to the fact that in this study the ring spacing was represented by a continuous variable and web and flange thicknesses were included as independent design variables, while in [3] the frame spacing was a discrete parameter and the web and flange thicknesses were linked and required to be not less than 1/18 of the web and flange depths. In the designs presented herein the frame webs are very thin and are critically stressed, i.e., on the verge of buckling. Consideration of lateral-torsional buckling and the effects of hull eccentricity may alter this condition, although these effects were excluded in the present work.

One important benefit in obtaining the minimum-weight designs in Table 1, is that they serve as initial, feasible designs for design problems II and III, provided the same minimum frequency constraint is employed and the maximum allowable structural mass is greater than that of the minimum-weight (mass) design for the static load conditions.

Table 1. Design Problem I - Weight Minimization

(R = 198 in., L = 594 in., E = 30 x 10^6 psi, σ_y = 60,000 psi)

Depth	1000 ft.	2000 ft.	3000 ft.
t_s, in.	1.2108	2.4856	3.5156
t_ϕ, in.	0.3765	0.4207	0.4543
d_ϕ, in.	19.589	19.284	19.915
ℓ_x, in.	33.602	51.528	36.195
d_f, in.	17.664	14.999	16.991
t_f, in.	0.4705	0.4984	0.5453
ω_1, Hz.	28.12	26.05	26.64
ω_2, Hz.	49.39	30.04	35.88
ω_3, Hz.	52.31	51.98	55.11
Weight[a] (Normalized)	0.13317	0.22295	0.31922

[a]Maximum (upper bound) weights (normalized) are 0.15, 0.25 and 0.35, respectively.

The results of design problem II, optimization for maximum frequency separation are given in Table 2 for the cases of the same three preassigned operating depths. The maximum allowable normalized weight was taken as approximately 10% greater than that for the minimum-weight design for the static load condition, the values being 0.15, 0.25 and 0.35, respectively, for the operating depths of 1000, 2000 and 3000 ft. For the three depth requirements the frequency separation was increased from the minimum-weight design values of 21.27, 3.993 and 9.2418 Hz to 23.59, 24.28 and 25.33 Hz. Of interest is the fact that the first and third solutions (for 1000 ft. and 3000 ft. operating depths) gave frequencies $\omega_2 = \omega_3$, i.e., nearly identical second and third frequencies, and that in these two cases the maximum weight constraint was less than critical. It is thus apparent that the major portion of the frequency separation is obtained by bringing the second frequency up to the third frequency, and that little or nothing is to be gained by adding more material to the structure after this is accomplished. In the example with 2000 ft. depth the second and third frequencies were unable to completely approach each other before violating the maximum weight constraint, which became critical in this case. It may be noted that for these designs the frame webs are very thin and the frame flanges are relatively thick. It thus seems that the frequency separation has been achieved by making the moment of inertia of the frames as large as possible.

Three problems of category III were designed to find the maximum frequency separation in primarily longitudinal modes of vibration for the three different operating depths. Results are given in Table 3. For the cases which have operating depths of 1000 ft. and 2000 ft. the algorithm became entrapped in a singularity in the design space. The problem run at 3000 ft. depth was unable to reach the singularity because the maximum weight

Table 2. Design Problem II - Frequency Separation

(R = 198 in., L = 594 in., E = 30 x 10^6 psi, σ_y = 60,000 psi)

Depth	1000 ft.	2000 ft.	3000 ft.
t_s, in.	1.2216	2.4717	3.3986
t_ϕ, in.	0.3950	0.3884	0.5168
d_ϕ, in.	20.722	19.674	23.764
ℓ_x, in.	33.853	51.417	36.065
d_f, in.	17.551	15.075	16.864
t_f, in.	0.4653	1.8638	0.9485
ω_1, Hz.	28.3711	29.4905	29.7225
ω_2, Hz.	51.9638	53.7674	55.0508
ω_3, Hz.	51.9640	54.1466	55.0512
Weight[a] (Normalized)	0.1351	0.25	0.32928
$(\omega_2-\omega_1)$ Hz.	23.5928	24.2769	25.3283

[a]Maximum (upper bound) weights (normalized) are 0.15, 0.25 and 0.35, respectively.

Table 3. Design Problem III - Longitudinal Frequency Separation

(R = 198 in., L = 594 in., E = 30 x 10^6 psi, σ_y = 60,000 psi)

Depth	1000 ft.	2000 ft.	3000 ft.
t_s, in.	1.5975	2.6720	3.9377
t_ϕ, in.	0.2500	0.4171	0.42116
d_ϕ, in.	11.603	17.384	19.817
ℓ_x, in.	38.672	52.232	36.143
d_f, in.	9.1454	13.232	16.907
t_f, in.	0.3826	0.5248	0.4927
ω_1, Hz.	163.0006	163.0640	138.2134
ω_2, Hz.	192.2375	192.7389	162.4559
ω_3, Hz.	222.6656	222.7126	221.6170
Weight[a] (Normalized)	0.14215	0.23559	0.34907
$(\omega_{L_2} - \omega_{L_1})$ Hz.	29.2369	29.6749	24.2425

[a]Maximum (upper bound) weights (normalized) are 0.15, 0.25, and 0.35, respectively.

constraint had become active. A singularity avoidance constraint could have been developed to enable the algorithm to proceed, however this was not done because in order for the optimization problem to have a significant physical purpose, a better definition of what actually constitutes a longitudinal mode is needed. As may be seen in Table 3 for the 3000 ft. case, the mode having one longitudinal wave and no circumference waves (m = 1, n = 0) has a "longitudinal" frequency of 138.21 Hz, because the v-component of the associated eigenvector is zero and the w-component is less than 1.0 (0.977). As the algorithm separates the frequencies, the eigenvector associated with this frequency changes form with the w-component increasing to a value slightly greater than 1.0. As this occurs, a second eigenvector of this mode's vibratory class (m = 1, n = 0) becomes longitudinal in form, according to the definition currently in use. The result is the situation encountered for the 1000 ft. and 2000 ft. cases, where the m = 1, n = 0 mode has the second lowest frequency. The algorithm becomes entrapped at a frequency separation of 29 Hz as two eigenvectors for the m = 1, n = 0 mode switch back and forth, having w-components both approximately equal to 1.0. Since the m = 1, n = 0 mode has two frequencies of vibration with almost the same mode shape it is not realistic to call either one the unique longitudinal frequency for that mode.

This effect was only recently encountered and must be given additional study. When successfully resolved, the result will be a capability for generating optimum solutions to design problems I, II and III. For the future, research should be directed toward incorporating more sophisticated structural models, with more design flexibility, in anticipation of obtaining even more efficient structural configurations from both the standpoint of minimum-weight and maximum frequency separation.

REFERENCES

1. Morrow, W.M., and Schmit, L.A., "Structural Synthesis of a Stiffened Cylinder," NASA CR-1217, December 1968.

2. Pappas, M., and Allentuch, A., "Structural Synthesis of Frame Reinforced Submersible, Circular, Cylindrical Hulls," NCE Report No. NV5, May 1972.

3. Pappas, M., and Allentuch, A., "Optimal Design of Submersible Frame Stiffened, Circular Cylindrical Hulls," NCE Report No. NV6 (Revised), July 1972.

4. Principles of Naval Architecture, Society of Naval Architects and Marine Engineers, New York, 1967.

5. Timoshenko, S.P., and Gere, J.M., Theory of Elastic Stability, 2nd Ed., McGraw-Hill, 1961.

6. Fox, R.L., Optimization Methods for Engineering Design, Addison-Wesley, 1971.

7. Kavlie, D., and Moe, J., "Automated Design of Frame Structures," Jour. of the Structural Division, ASCE, Vol. 97, No. ST1, Jan. 1971, pp. 33-62.

APPENDIX I: DYNAMIC ANALYSIS

The forces on the cylindrical shell are as shown in Fig. 2. The forces are expressed in terms of displacements as:

$$N_x = Hu' + (H\nu/R)v^* - (H\nu/R)w + (D/R)w''$$

$$N_\phi = H\nu u' + [(H+HC+HF)/R]v^* - [H+HC(1+e_\phi/R) + HF(1+e_f/R)]w/R$$

$$- [D/R+HC(e_\phi+\rho_\phi^2/R) + HF(e_f+\rho_f^2/R)]\frac{1}{R^2}\, w^{**}$$

$$N_{x\phi} = (S/R)u^* + Sv' + (K/R^2)w'^*$$

$$N_{\phi x} = (S/R)u^* + Sv' - (K/R^2)w'^*$$

$$M_x = - (D/R)u' - (D\nu/R^2)v^* - Dw'' - (D\nu/R^2)w^{**}$$

$$M_\phi = (HCe_\phi/R + HFe_f/R)v^* - [D/R + HC(e_\phi+\rho_\phi^2/R) + HF(e_f+\rho_f^2/R)]w/R$$

$$- D\nu w'' - [D + HC(\rho_\phi^2+\alpha_\phi^3/R) + HF(\rho_f^2+\alpha_f^2/R)w^{**}/R$$

$$M_{x\phi} = - (2K/R)(v'+w'^*)$$

$$M_{\phi x} = (K/R^2)u^* - (K/R)v' - (2K+Q)w'^*/R$$

$$(\,)^* = \frac{\partial(\,)}{\partial\phi}\,,\quad (\,)' = \frac{\partial(\,)}{\partial x}$$

The matrices [K], [K_G] and [M] of equation (6) are:

$$[K] = \begin{bmatrix} k_{11} & k_{12} & k_{13} \\ k_{12} & k_{22} & k_{23} \\ k_{13} & k_{23} & k_{33} \end{bmatrix}$$

$$k_{11} = - H\lambda^2 - (S/R^2)n^2$$

$$k_{12} = - (H\nu+S)\lambda n/R$$

$$k_{13} = - [H\nu\lambda+D\lambda^3 - (K/R^2)\lambda n^2]/R$$

$$k_{22} = - (S+2K/R^2)\lambda^2 - [H+HC(1-e_\phi/R) + HF(1-e_f/R)]n^2/R^2$$

$$k_{23} = -(3K+D\nu)\lambda^2 n/R^2$$

$$+ [D/R^2-H+HC(\rho_\phi^2/R^2-1) + HF(\rho_f^2/R^2-1)]n/R^2$$

$$- [HC(\alpha_\phi^3/R^2-e_\phi) + HF(\alpha_f^3/R^2-e_f)]n^3/R^3$$

$$k_{33} = -[H+HC(1+e_\phi/R) + HF(1+e_f/R)]/R^2$$

$$+ 2[D/R+HC(e_\phi+\rho_\phi^2/R) + HF(e_f+\rho_f^2/R)]n^2/R^3$$

$$- D\lambda^4 - [2D\nu+4K+Q](\lambda n/R)^2$$

$$- [D+HC(\rho_\phi^2+\alpha_\phi^3/R) + HF(\rho_f^2+\alpha_f^3/R)](n/R)^4$$

$$[K_G] = \begin{bmatrix} k_{G11} & 0 & k_{G13} \\ 0 & k_{G22} & k_{G23} \\ k_{G13} & k_{G23} & k_{G33} \end{bmatrix}$$

$$k_{G11} = -(n^2+\lambda^2/2)/R \qquad k_{G23} = n/R$$

$$k_{G13} = -\lambda \qquad k_{G33} = -(n^2+\lambda^2/2)/R$$

$$k_{G22} = -(n^2+\lambda^2/2)/R$$

$$M = \begin{bmatrix} m_{11} & 0 & m_{13} \\ 0 & m_{22} & m_{23} \\ m_{13} & m_{23} & m_{33} \end{bmatrix}$$

$$m_{11} = t_s + A(1-e_\phi/R) + B(1-e_f/R)$$

$$m_{13} = [t_s^3/(12R) + A(-e_\phi+\rho_\phi^2/R) + B(-e_f+\rho_f^2/R)]\lambda$$

$$m_{22} = t_s\left(1 + \frac{t_s^2}{4R^2}\right) + A(1-3e_\phi/R+3\rho_\phi^2/R^2-\alpha_\phi^3/R^3)$$

$$+ B(1-3e_f/R+3\rho_f^2/R^2-\alpha_f^3/R^3)$$

$$m_{23} = [t_s^3/(6R^2) + A(-e_\phi/R+2\rho_\phi^2/R^2-\alpha_\phi^3/R^3)$$

$$+ B(-e_f/R+2\rho_f^2/R^2-\alpha_f^3/R^3)]n$$

$$m_{33} = t_s + (\lambda^2+n^2/R^2)t_s^3/12 + A[1-e_\phi/R + (\lambda^2+n^2/R^2)(\rho_\phi^2-\alpha_\phi^3/R)]$$

$$+ B[1-e_f/R+(\lambda^2+n^2/R^2)(\rho_f^2-\alpha_f^3/R)]$$

The section properties are defined as follows:

$H = Et_s/(1-\nu^2)$ $\qquad$ $D = Et_s^3/[12(1-\nu^2)]$

$A = t_\phi d_\phi/\ell_x$ $\qquad$ $B = t_f d_f/\ell_x$

$HC = EA$ $\qquad$ $HF = EB$

$G = E/[2(1+\nu)]$ $\qquad$ $t_t = t_s + 2d_\phi$

$S = Gt_s$ $\qquad$ $K = Gt_s^3/12$

$Q = G(J_\phi+J_f)\ell_x$

$J_\phi = c_\phi d_\phi t_\phi^3$ $\qquad$ $c_\phi = -0.285\, e^{-\left(0.49\,\frac{d_\phi}{t_\phi}\right)} + 0.316$

$J_f = c_f d_f t_f^3$ $\qquad$ $c_f = -0.285\, e^{-\left(0.49\,\frac{d_f}{t_f}\right)} + 0.316$

$e_\phi = \frac{1}{2}(d_\phi+t_s)$ $\qquad$ $e_f = \frac{1}{2}(d_f+t_t)$

$$\rho_\phi^2 = \frac{1}{3}d_\phi^2 + \frac{1}{2}d_\phi t_s + \frac{1}{4}t_s^2$$

$$\rho_f^2 = \frac{1}{3}d_f^3 + \frac{1}{2}d_f t_t + \frac{1}{4}t_t^2$$

$$\alpha_\phi^3 = \frac{1}{4}d_\phi^3 + \frac{1}{2}t_s d_\phi^2 + \frac{3}{8}t_s^2 d_\phi + \frac{1}{8}t_s^3$$

$$\alpha_f^3 = \frac{1}{4}d_f^3 + \frac{1}{2}t_t d_f^2 + \frac{3}{8}t_t^2 d_f + \frac{1}{8}t_s^3$$

APPENDIX II: STATIC STRENGTH ANALYSIS

The critical compressive stresses in the skin are assumed to occur on the outer surface at mid panel. The stresses there are

$$\sigma_\phi = - (PR/t_s)[1+\Gamma(H_n+\nu H_E)]$$

$$\sigma_x = - (PR/t_s)[\tfrac{1}{2} + \Gamma H_E]$$

where the various parameters are given as:

$-PR/t_s$ = hoop stress

R = radius to mid plane of shell

$\Gamma = [1-\nu/2-B]/(1+\beta)$

B = ratio of shell area under frame web to total frame area = $t_s t_\phi/A$

$A = t_s t_\phi + t_\phi d_\phi + t_f d_f$

$\beta = 2N\{1/[3(1-\nu^2)]\}^{1/4}(Rt_s^3)^{1/2}/A$

$N = (\cosh\theta-\cos\theta)/(\sinh\theta+\sin\theta)$

$\theta = \ell[3(1-\nu^2)/(Rt_s)^2]^{1/4}$

ℓ = unsupported length of shell = $\ell_x - t_\phi$

$H_n = - 2[\sinh(\theta/2)\cos(\theta/2)+\cosh(\theta/2)\sin(\theta/2)]/(\sinh\theta+\sin\theta)$

$H_E = - 2[3/(1-\nu^2)]^{1/2}[\sinh(\theta/2)\cos(\theta/2)-\cosh(\theta/2)\sin(\theta/2)]/(\sinh\theta+\sin\theta)$

The hoop compressive stress in the frame is

$$\sigma_c = PVR/A$$

where V is a load factor given as:

$$V = t_\phi[1+(1-\nu/2)\beta/B]/(1+\beta)$$

Distribution List

Chief of Naval Research
Department of the Navy
Arlington, Virginia 22217
Attn: Code 439 (2)
471

Director
ONR Branch Office
495 Summer Street
Boston, Massachusetts 02210

Director
ONR Branch Office
219 S. Dearborn Street
Chicago, Illinois 60604

Director
Naval Research Laboratory
Attn: Library, Code 2029 (ONRL)
Washington, D.C. 20390 (6)

Commanding Officer
ONR Branch Office
207 West 24th Street
New York, New York 10011

Director
ONR Branch Office
1030 E. Green Street
Pasadena, California 91101

U. S. Naval Research Laboratory
Attn: Technical Information Div.
Washington, D.C. 20390 (6)

Defense Documentation Center
Cameron Station
Alexandria, Virginia 22314 (20)

Army

Commanding Officer
U.S. Army Research Office Durham
Attn: Mr. J.J. Murray
CRD-AA-IP
Box CM, Duke Station
Durham, North Carolina 27706

Commanding Officer
AMXMR-ATL
Attn: Mr. J. Bluhm
U.S. Army Materials Res. Agcy.
Watertown, Massachusetts 02172

Watervliet Arsenal
MAGGS Research Center
Watervliet, New York 12189
Attn: Director of Research

Redstone Scientific Info. Center
Chief, Document Section
U.S. Army Missile Command
Redstone Arsenal, Alabama 35809

Army R & D Center
Fort Belvoir, Virginia 22060

Technical Library
Aberdeen Proving Ground
Aberdeen, Maryland 21005

Navy

Commanding Officer and Director
Naval Ship Research & Development Center
Washington, D.C. 20007
Attn: Code 042 (Tech. Lib. Br.)
700 (Struc. Mech. Lab.)
720
725
727
012.2 (dr. W.J. Sette)

Naval Weapons Laboratory
Dahlgren, Virginia 22448

Naval Research Laboratory
Washington, D.C. 20390
Attn: Code 8400
8410
8430
8440
6300
6305
6380

Undersea Explosion Research Div.
Naval Ship R & D Center
Norfolk Naval Shipyard
Portsmouth, Virginia 23709
Attn: Dr. Schauer
Code 780

Naval Ship R & D Center
Annapolis Division
Annapolis, Maryland 21402
Attn: Code A800, Mr. W. L. Williams

Technical Library
Naval Underwater Weapons Center
Pasadena Annex
3202 East Foothill Blvd.
Pasadena, California 91107

U.S. Naval Weapons Center
China Lake, California 93557
Attn: Code 4520 Mr. Ken Bischel

U.S. Naval Ordnance Laboratory
Mechanics Division
RFD 1, White Oak
Silver Spring, Maryland 20910

U.S. Naval Ordnance Laboratory
Attn: Mr. H. A. Perry, Jr.
Non-Metallic Materials Division
Silver Spring, Maryland 20910

Technical Director
U.S. Naval Undersea R & D Center
San Diego, California 92132

Supervisor of Shipbuilding
U.S. Navy
Newport News, Virginia 23607

Technical Director
Mare Island Naval Shipyard
Vallejo, California 94594

U.S. Naval Ordnance Station
Attn: Mr. Garet Bornstein
Research & Development Division
Indian Head, Maryland 20640

Chief of Naval Operations
Department of the Navy
Washington, D.C. 20350
Attn: Code OP-07T

Deep Submergence Systems
Naval Ship Systems Command
Code 39522
Department of the Navy
Washington, D.C. 20360
Attn: Chief Scientist

Director, Aero Mechanics
Naval Air Development Center
Johnsville
Warminster, Pennsylvania 18974

Naval Air Systems Command
Department of the Navy
Washington, D.C. 20360
Attn: NAIR 320 Aero & Structures
5320 Structures
604 Tech. Library
52031F Materials

Naval Facilities Engineering Command
Department of the Navy
Washington, D.C. 20360
Attn: NFAC 03 Res. & Development
04 Engineering & Design
14114 Tech. Library

Naval Ship Systems Command
Department of the Navy
Washington, D.C. 20360
Attn: NSHIP 031 Ch. Scientists for R & D
0342 Ship Mats. & Structs.
2052 Tech. Library

Naval Ship Engineering Center
Prince George Plaza
Hyattsville, Maryland 20782
Attn: NSEC 6100 Ship Sys. Engr. & Des.
6102C Computer-Aided Ship Des.
6105 Ship Protection
6110 Ship Concept Design
6120 Hull Div.
6120D Hull Div.
6128 Surface Ship Struct.
6129 Submarine Struct.

Naval Ordnance Systems Command
Department of the Navy
Washington, D.C. 20360
Attn: NORD 03 Res. & Technology
035 Weapons Dynamics
9132 Tech. Library

Engineering Department
U.S. Naval Academy
Annapolis, Maryland 21402

Air Force

Commander WADD
Wright-Patterson Air Force Base
Dayton, Ohio 45433
Attn: Code WWRMDD
AFFDL (FDDS)
Structures Division
AFLC (MCEEA)
Code WWRC
AFML (MAAM)

Commander
Chief, Applied Mechanics Group
U.S. Air Force Inst. of Tech.
Wright-Patterson Air Force Base
Dayton, Ohio 45433

Chief, Civil Engineering Branch
WLRC, Research Division
Air Force Weapons Laboratory
Kirtland AFB, New Mexico 87117

Air Force Office of Scientific Res.
1400 Wilson Blvd.
Arlington, Virginia 22209
Attn: Mechs. Div.

NASA

Structures Research Division
National Aeronautics and Space Admin.
Langley Research Center
Langley Station
Hampton, Virginia 23365
Attn: Mr. R.R. Heldenfels, Chief

National Aeronautics & Space Admin.
Associate Administrator for Advanced
Research & Technology
Washington, D.C. 20546

Scientific & Tech. Info. Facility
NASA Representative (S-AK/DL)
P.O. Box 5700
Bethesda, Maryland 20014

Other Government Activities

Technical Director
Marine Corps Development & Educ. Command
Quantico, Virginia 22134

Director
National Bureau of Standards
Washington, D.C. 20234
Attn: Mr. B.L. Wilson, EM 219

National Science Foundation
Engineering Division
Washington, D.C. 20550

Director
STBS
Defense Atomic Support Agency
Washington, D.C. 20350

Commander Field Command
Defense Atomic Support Agency
Sandia Base
Albuquerque, New Mexico 87115

Chief, Defense Atomic Support Agcy.
Blast & Shock Division
The Pentagon
Washington, D.C. 20301

Director Defense Research & Engr.
Technical Library
Room 3C-128
The Pentagon
Washington, D.C. 20301

Chief, Airframe & Equipment
FS-120
Office of Flight Standards
Federal Aviation Agency
Washington, D.C. 20553

Chief of Research and Development
Maritime Administration
Washington, D.C. 20235

Mr. Milton Shaw, Director
Div. of Reactor Develop. & Technology
Atomic Energy Commission
Germantown, Maryland 20767

Ship Hull Research Committee
National Research Council
National Academy of Sciences
2101 Constitution Avenue
Washington, D.C. 20418
Attn: Mr. A.R. Lytle

PART 2 - CONTRACTORS AND OTHER TECHNICAL COLLABORATORS

Universities

Professor J.R. Rice
Division of Engineering
Brown University
Providence, Rhode Island 02912

Dr. J. Tinsley Oden
Dept. of Engr. Mechs.
University of Alabama
Huntsville, Alabama 35804

Professor R.S. Rivlin
Center for the Application of Mathematics
Lehigh University
Bethlehem, Pennsylvania 18015

Professor Julius Miklowitz
Div. of Engr. & Applied Sciences
California Institute of Technology
Pasadena, California 91109

Professor George Sih
Department of Mechanics
Lehigh University
Bethlehem, Pennsylvania 18015

Dr. Harold Liebowitz, Dean
School of Engrg. & Applied Science
George Washington University
725 23rd Street
Washington, D.C. 20006

Professor Eli Sternberg
Div. of Engrg. & Applied Sciences
California Institute of Technology
Pasadena, California 91109

Professor Burt Paul
University of Pennsylvania
Towne School of Civil & Mech. Engrg.
Room 113 Towne Building
220 So. 33rd Street
Philadelphia, Pennsylvania 19104

Professor S.B. Dong
University of California
Department of Mechanics
Los Angeles, California 90024

Professor Paul M. Naghdi
Div. of Applied Mechanics
Etcheverry Hall
University of California
Berkeley, California 94720

Professor W. Nachbar
University of California
Dept. of Aerospace & Mech. Engrg.
La Jolla, California 92037

Professor J. Baltrukonis
Mechanics Division
The Catholic Univ. of America
Washington, D.C. 20017

Professor A.J. Durelli
Mechanics Division
The Catholic Univ. of America
Washington, D.C. 20017

Professor H.H. Bleich
Dept. of Civil Engineering
Columbia University
Amsterdam & 120th Street
New York, New York 10027

Professor R.D. Mindlin
Dept. of Civil Engineering
Columbia University
S.W. Mudd Building
New York, New York 10027

Professor A.M. Freudenthal
George Washington University
School of Engrg. & Applied Science
Washington, D.C. 20006

Professor B.A. Boley
Dept. of Theoretical & Applied Mechanics
Cornell University
Ithaca, New York 14850

Professor P.G. Hodge
Department of Mechanics
Illinois Institute of Technology
Chicago, Illinois 60616

Dr. D.C. Drucker
Dean of Engineering
University of Illinois
Urbana, Illinois 61801

Professor N.M. Newmark
Dept. of Civil Engineering
University of Illinois
Urbana, Illinois 61801

Professor James Mar
Massachusetts Institute of Technology
Room 33-318
Dept. of Aerospace & Astro.
77 Massachusetts Avenue
Cambridge, Massachusetts 02139

Library (Code 0384)
U.S. Naval Postgraduate School
Monterey, California 93940

Dr. Francis Cozzarelli
Div. of Interdisciplinary Studies & Research
School of Engineering
State University of New York
Buffalo, New York 14214

Professor R.A. Douglas
Dept. of Engrg. Mechs.
North Carolina State University
Raleigh, North Carolina 27607

Dr. George Herrmann
Stanford University
Dept. of Applied Mechanics
Stanford, California 94305

Professor J.D. Achenbach
Technological Institute
Northwestern University
Evanston, Illinois 60201

Director, Ordnance Research Lab.
Pennsylvania State University
P.O. Box 30
State College, Pennsylvania 16801

Professor J. Kempner
Dept. of Aero Engrg. & Applied Mech.
Polytechnic Institute of Brooklyn
333 Jay Street
Brooklyn, New York 11201

Professor J. Klosner
Polytechnic Institute of Brooklyn
333 Jay Street
Brooklyn, New York 11201

Professor A.C. Eringen
Dept. of Aerospace & Mech. Sciences
Princeton University
Princeton, New Jersey 08540

Dr. S.L. Koh
School of Aero., and Engrg. Sci.
Purdue University
Lafayette, Indiana 47907

Professor R.A. Schapery
Civil Engineering Department
Texas A & M University
College Station, Texas 77840

Professor E.H. Lee
Div. of Engrg. Mechanics
Stanford University
Stanford, California 94305

Dr. Nicholas J. Hoff
Dept. of Aero. & Astro.
Stanford University
Stanford, California 94305

Professor Max Anliker
Dept. of Aero & Astro.
Stanford University
Stanford,California 94305

Professor Chi-Chang Chao
Div. of Engrg. Mechanics
Stanford University
Stanford, California 94305

Professor H.W. Liu
Dept. of Chemical Engrg. and Metal.
Syracuse University
Syracuse, New York 13210

Professor S. Bodner
Technion R & D Foundation
Haifa, Israel

Dr. S. Dhawan, Director
Indian Institute of Science
Bangalore, India

Professor Tsuyoshi Hayashi
Department of Aeronautics
Faculty of Engineering
University of Tokyo
BUNKYO-KU
Tokyo, Japan

Professor J.E. Fitzgerald, Ch.
Dept. of Civil Engineering
University of Utah
Salt Lake City, Utah 84112

Professor R.J.H. Bollard
Chairman, Aeronautical Engrg. Dept.
207 Guggenheim Hall
University of Washington
Seattle, Washington 98105

Professor Albert S. Kobayashi
Dept. of Mechanical Engrg.
University of Washington
Seattle, Washington 98105

Professor G.R. Irwin
Dept. of Mech. Engrg.
Lehigh University
Bethlehem, Pennsylvania 18015

Dr. Daniel Frederick
Dept. of Engrg. Mechs.
Virginia Polytechnic Inst.
Blacksburg,Virginia 24061

Professor Lambert Tall
Lehigh University
Department of Civil Engrg.
Bethlehem, Pennsylvania 18015

Professor M.P. Wnuk
South Dakota State University
Department of Mechanical Engineering
Brookings, South Dakota 57006

Professor Norman Jones
Massachusetts Institute of Technology
Dept. of Naval Architecture & Marine Engrg.
Cambridge, Massachusetts 02139

Professor Pedro V. Marcal
Brown University
Division of Engineering
Providence, Rhode Island 02912

Professor Werner Goldsmith
Department of Mechanical Engineering
Division of Applied Mechanics
University of California
Berkeley, California 94720

Professor R.B. Testa
Dept. of Civil Engrg.
Columbia University
S.W. Mudd Bldg.
New York, New York 10027

Dr. Y. Weitsman
Dept. of Engrg. Sciences
Tel-Aviv University
Ramat-Aviv
Tel-Aviv, Israel

Professor W.D. Pilkey
Dept. of Aerospace Engrg.
University of Virginia
Charlottesville, Virginia 22903

Professor W. Prager
Division of Engineering
Brown University
Providence, Rhode Island 02912

Industry and Research Institutes

Mr. Carl E. Hartbower
Dept. 4620, Bldg. 2019 A2
Aerojet-General Corporation
P.O. Box 1947
Sacramento, California 95809

Library Services Department
Report Section, Bldg. 14-14
Argonne National Lab.
9400 S. Cass Avenue
Argonne, Illinois 60440

Dr. F. R. Schwarzl
Central Laboratory T.N.O.
Schoemakerstraat 97
Delft, The Netherlands

Dr. Wendt
Valley Forge Space Technology Cen.
General Electric Co.
Valley Forge, Pennsylvania 10481

Library Newport News Shipbuilding
& Dry Dock Company
Newport News, Virginia 23607

Director
Ship Research Institute
Ministry of Transportation
700, SHINKAWA
Mitaka
Tokyo, Japan

Dr. H.N Abramson
Southwest Research Institute
8500 Culebra Road
San Antonio, Texas 78206

Dr. R.C. DeHart
Southwest Research Institute
8500 Culebra Road
San Antonio, Texas 78206

Mr. Roger Weiss
High Temp. Structures & Materials
Applied Physics Lab.
8621 Georgia Avenue
Silver Spring, Maryland 20910

Mr. E.C. Francis, Head
Mech. Props. Eval.
United Technology Center
Sunnyvale, California 94088

Mr. C.N. Robinson
Atlantic Research Corp.
Shirley Highway at Edsall Road
Alexandria, Virginia 22314

Mr. P.C. Durup
Aeromechanics Dept., 74-43
Lockheed-California Co.
Burbank, California 91503

Mr. D. Wilson
Litton Systems, Inc.
AMTD, Dept. 400
El Segundo
9920 W. Jefferson Blvd.
Culver City, California 90230

Dr. Kevin J. Forsberg, Head
Solid Mechanics
Orgn 52-20, Bldg. 205
Lockheed Palo Alto Research Lab.
Palo Alto, California 94302

Dr. E.M.Q. Roren, Head
Research Department
Det Norske Veritas
Post Box 6060
Oslo, Norway

Dr. Andrew F. Conn
Hydronautics, Incorporated
Pindell School Road, Howard County
Laurel, Maryland 20810